

# Investigator atmospheric fronts summary

Andrew Brown

IN2023 V06, October 2023

## 1 Introduction

There were four synoptic-scale atmospheric fronts observed throughout the voyage “Understanding Eddy Interactions and their Impacts in the East Australian Current” (IN2023 V06, 9th October – 2nd November). Each of these fronts were associated with a southerly change behind northerly winds (so-called ”southerly busters” in this region). These are described here in order of their occurrence, using underway observations from Investigator meteorological sensors, radiosonde-derived atmospheric profiles, and radar reflectivity scans from the onboard weather radar (Ocean-POL or OPOL).

## 2 First front, 12/10/2023 13:22 UTC

The research vessel Investigator was located within relatively warm SSTs within the EAC during the first frontal passage, exceeding 22 degrees Celsius (location number 3 on Figure 1). A sudden change in wind direction and temperature drop of around 2 degrees was observed at 13:22 UTC (Figure 2), extending to a 3 degree temperature drop 5 minutes later. There is no clear wind speed increase or pressure drop associated with the front, suggesting a lack of strong convective outflow. Instead, the wind gust speed decreases during the frontal passage and strengthens in the post frontal air mass, reaching a maximum of 53 kts at around 15:00 UTC. A linear precipitation system was observed at 13:24 UTC by the onboard OPOL radar associated with the front (Figure 3), consistent with large amounts of convective available potential energy (CAPE) in the pre-frontal sounding (Figure 4). However, there was only small amounts of precipitation observed by the Investigator (0.2–0.6 mm).

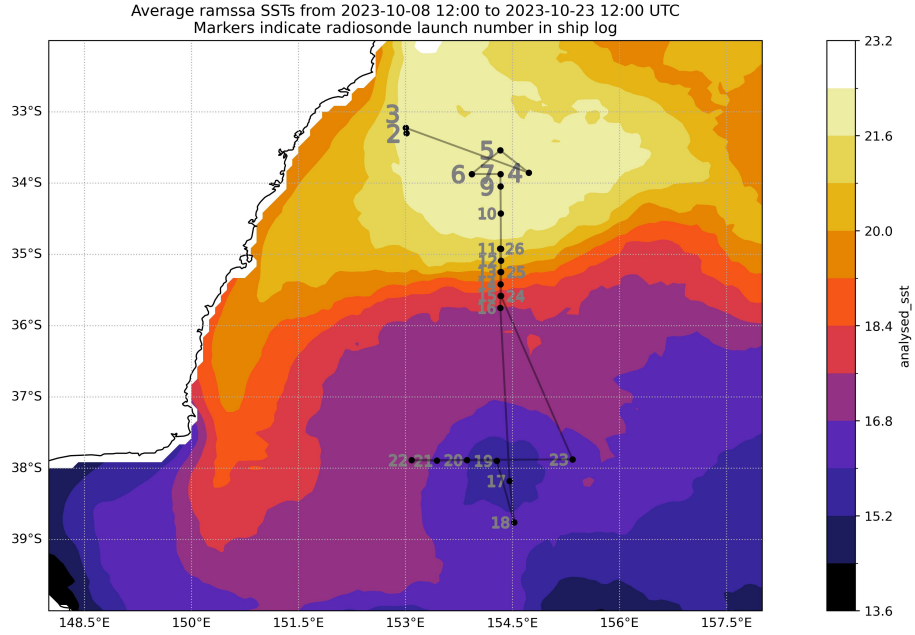


Figure 1: Map of radiosonde launch locations. Numbered according to the IN2023 V06 voyage log. Average RAMSSA SSTs are coloured.



Figure 2: Time series of first frontal passage from onboard meteorological sensors

2023-10-12T13:24:32

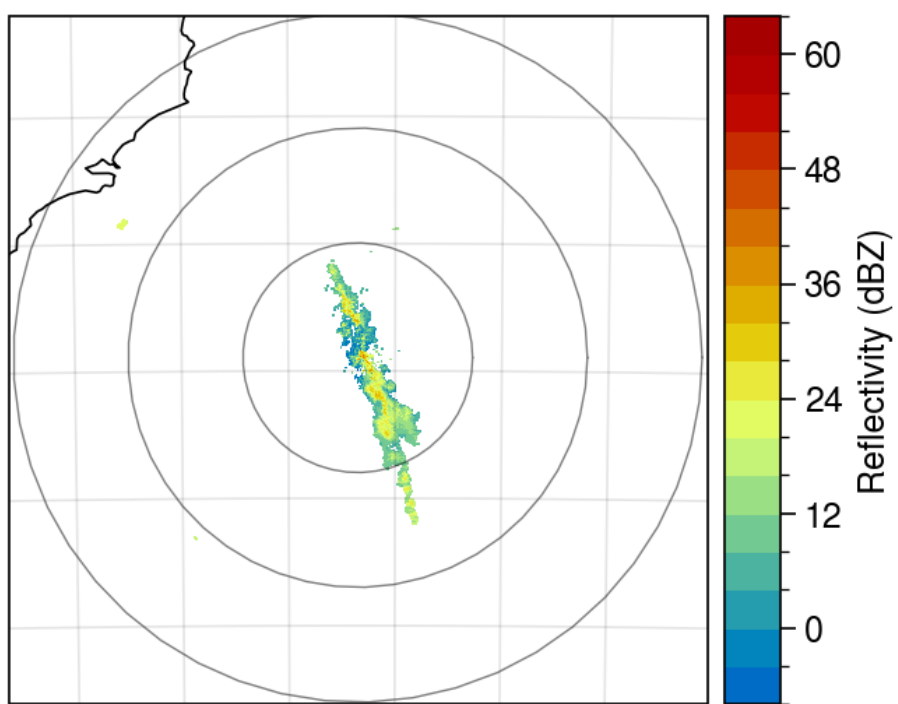


Figure 3: Radar reflectivity from second-lowest OPOL scan. Time in UTC.

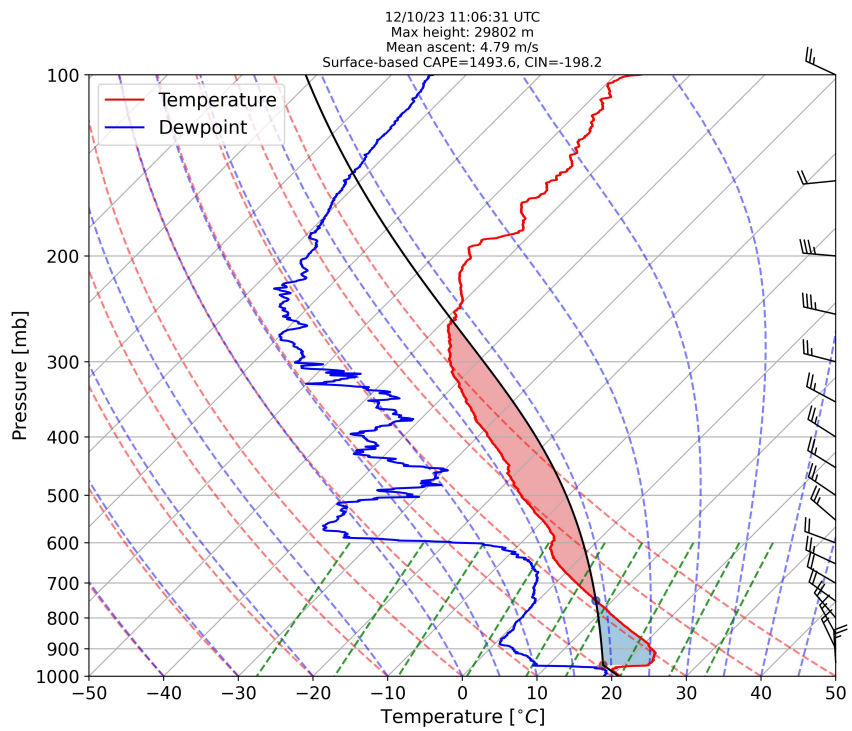


Figure 4: Observed radiosonde-derived sounding, around 2 hours prior to the first frontal passage. CAPE, CIN, and mean balloon ascent rate are indicated.

### 3 Second front 16/10/2023 03:35 UTC

The second front passed the ship location on the cold side of a strong oceanic front (location 16 on Figure 1). Again, a sudden change in wind direction is observed, with an initial temperature drop of 4 degrees Celsius, extending to a 6 degree drop around 15 minutes later. Together with a sudden wind gust spike (from 20 kts to 63 kts), and a pressure surge followed by sudden drop (rise in 1 hPa followed by a 5 hPa drop), this suggests that convection was embedded within the front, resulting in strong outflow being observed at the surface<sup>1</sup>. The OPOL radar also shows this convection embedded within the front (Figure 6), and the sounding in Figure 7 shows 540 J/kg of CAPE, 4 hours before the frontal passage. Satellite images suggest cloud tops around -40 to -50 degrees Celsius (Figure 8), with lightning also observed (not shown). Further analysis of this front, including relating the peak gust to downdraft processes using the vertical wind profile and surface observations (Nakamura et al. 1998), can be found in the Appendix.

---

<sup>1</sup>If precipitation falls out of a cloud into a relatively dry layer, evaporative cooling can make the air negatively buoyant compared with its environment. Together with the weight of the precipitation, this causes the air to accelerate towards the surface (downdraft). When the downdraft meets the surface, it can spread out horizontally and create strong wind gusts. The relatively cold air that pools at the surface ("outflow") is measured as a sudden temperature drop, while an increase in pressure is caused by a build-up of air impacting the surface.

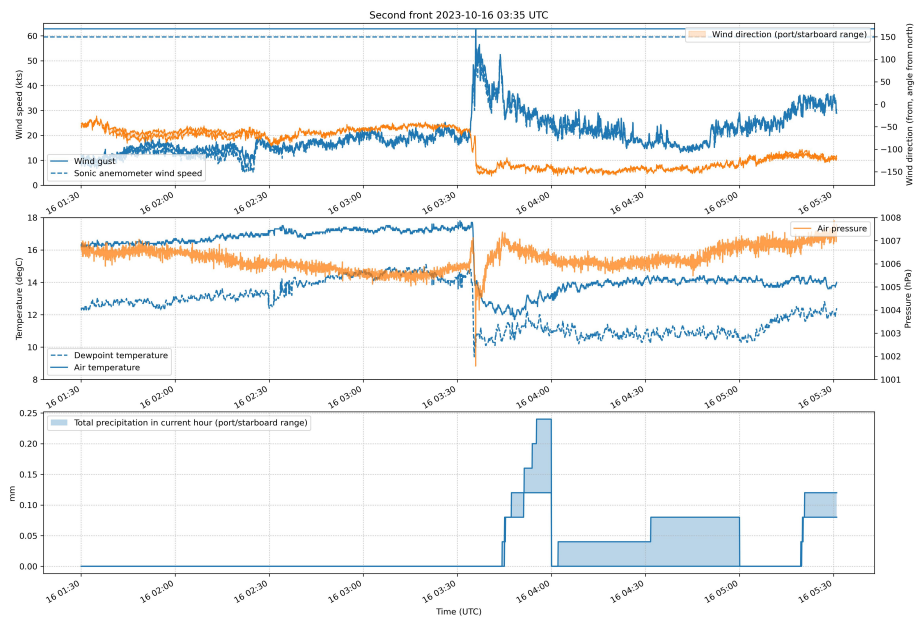


Figure 5: Time series of second frontal passage from onboard meteorological sensors

2023-10-16T03:36:32

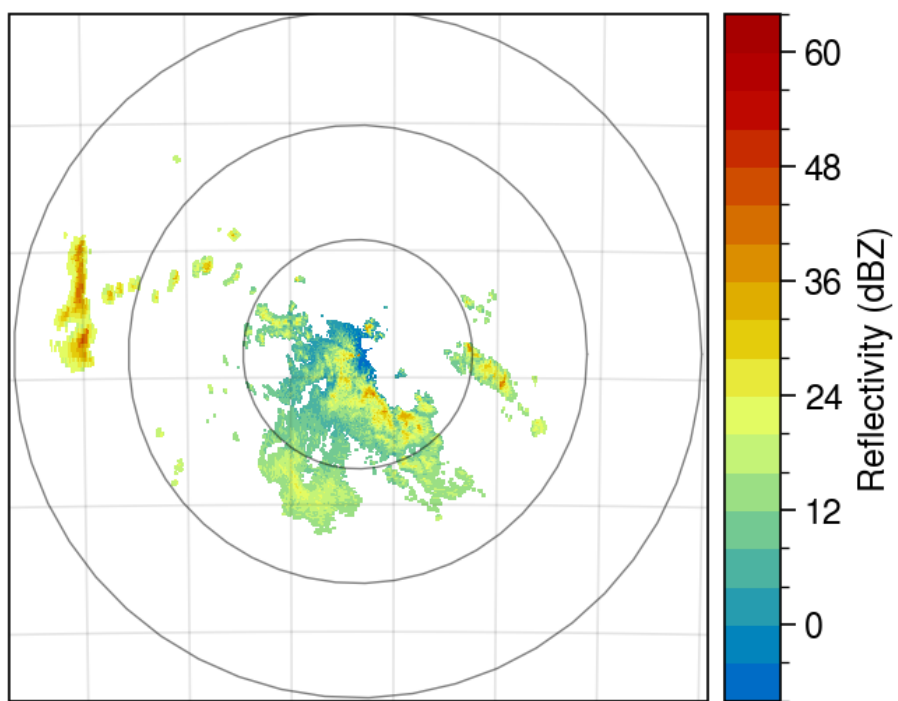


Figure 6: Radar reflectivity from second-lowest OPOL scan. Time in UTC.

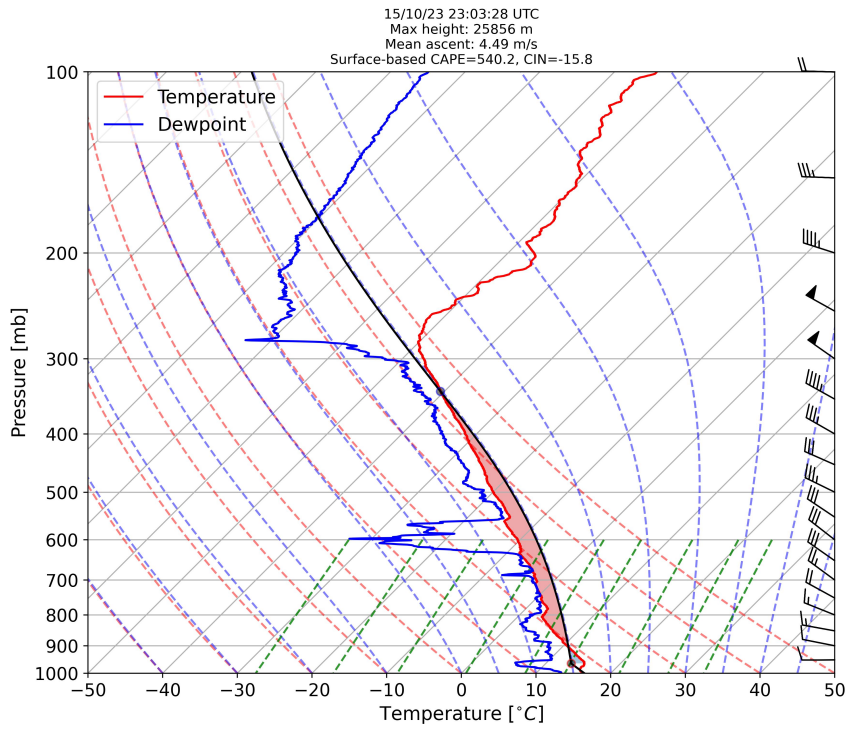


Figure 7: Observed radiosonde-derived sounding, around 4 hours prior to the second frontal passage. CAPE, CIN, and mean balloon ascent rate are indicated.

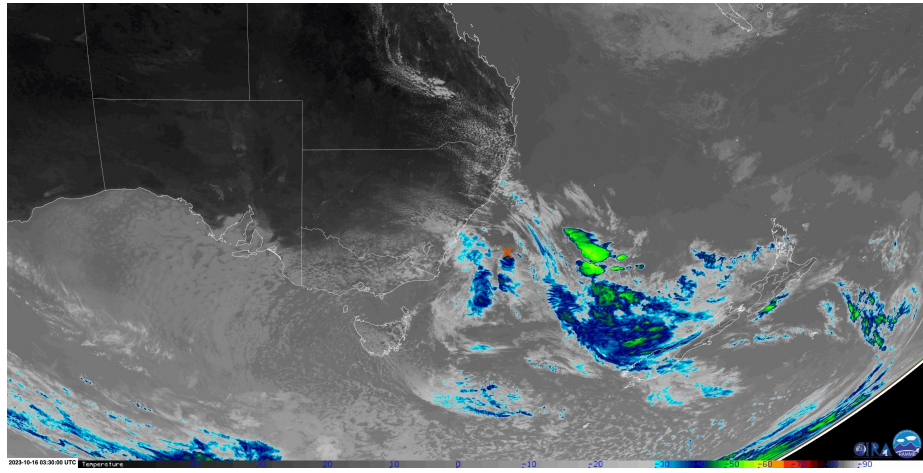


Figure 8: Satellite image at 0330 UTC from Himawari. From CIRA RAMMB satellite viewer. Approximate ship location marked with an orange cross.



Figure 9: Time series of third frontal passage from onboard meteorological sensors

## 4 Third front 22/10/2023 05:25 UTC

This front was observed by the ship located south of an oceanic front (between locations 24 and 25 on Figure 1). The front was associated with an extratropical cyclone centred over Tasmania. Similar to the first frontal passage, a change in wind speed is accompanied by a sudden temperature drop, although without a spike in wind gust speeds or sudden pressure increase (Figure 9), suggesting that there were no convective processes present. Minimal CAPE was present 5 hours prior to the frontal passage, with significant CIN (Figure 10).

## 5 Fourth front 25/10/2023 09:00 UTC

This front was accompanied by a drop in temperature of 2 degrees, with no change in wind speed, and shift to southerly winds. There was also very little rainfall associated with the frontal passage. This front was observed while the investigator was in relatively warm East Australian Current water (SST of around 22 degrees).

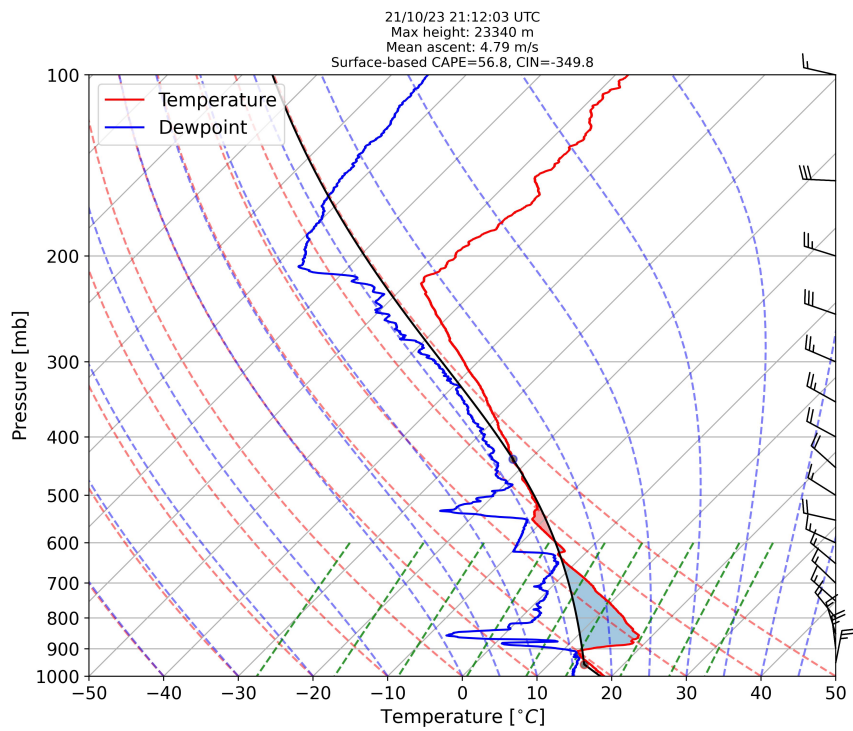


Figure 10: Observed radiosonde-derived sounding, around 5 hours prior to the third frontal passage. CAPE, CIN, and mean balloon ascent rate are indicated.

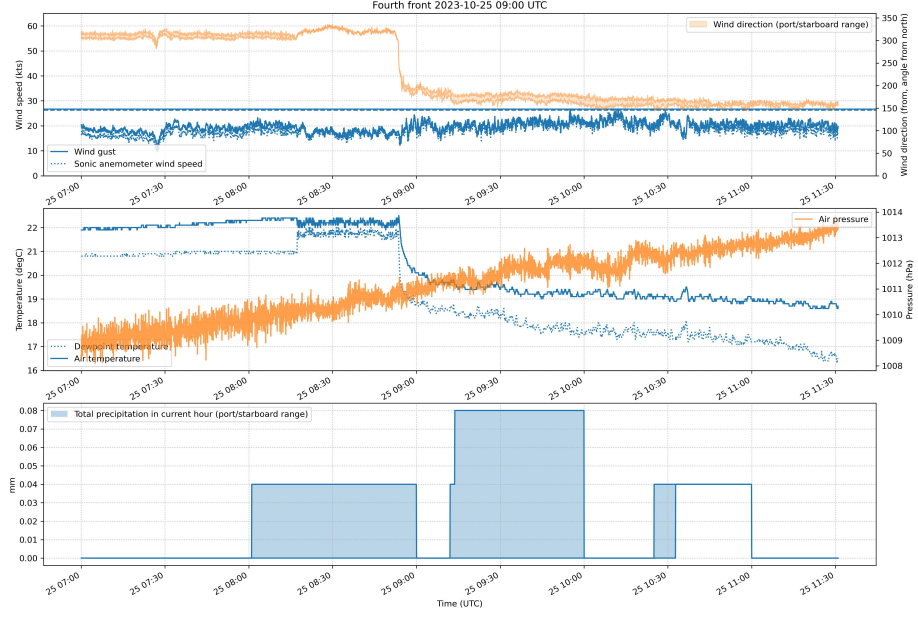


Figure 11: Time series of fourth frontal passage from onboard meteorological sensors

## 6 Conclusion

Four synoptic-scale atmospheric fronts were observed during IN2023 V06. Three of these fronts were associated purely with synoptic-scale processes at the surface, while the second front had embedded convection that produced strong outflow and a wind gust peak at the surface (63 kts or 117 km/hr). It is unclear whether the underlying SSTs played a role in the strength of the convective gust.

## References

- Nakamura, K., Kershaw, R., & Gait, N. (1996). Prediction of near-surface gusts generated by deep convection. *Meteorological Applications*, 3(2), 157–167. <https://doi.org/https://doi.org/10.1002/met.5060030206>

## Appendix

### Relating the second front peak gust to downdraft processes

Nakamura et al. (1998) note that convective wind gusts at the surface are driven by a combination of downdraft buoyancy processes, including evaporative cooling and precipitation loading, and downwards transport of horizontal momentum from aloft to the surface. For convection embedded within synoptic-scale systems, such as the frontal passage discussed here, downwards momentum transport is likely a significant factor. Nakamura et al. (1998) describe the following estimate of surface wind gust speed:

$$V_{gust} = \sqrt{\int_0^H 2g \left( \frac{\Delta\theta}{\theta} + q_r \right) dz + V(H)^2} \quad (1)$$

where  $\theta$  is the potential temperature of the environment,  $\Delta\theta$  is the potential temperature deficit of descending air,  $H$  is the initial height of a convective downdraft,  $q_r$  is the rain water mixing ratio within the downdraft, and  $V(H)$  is the initial horizontal wind speed of the downdraft. The first term of this equation represents an estimate of the buoyancy component of the surface gust, while the second term represents an estimate of downwards horizontal momentum transport. Nakamura et al. (1998) also describe a simplification of this equation, that can be calculated based on surface observations and the vertical wind profile:

$$V_{gust} = \sqrt{g \frac{\Delta T_s}{T} H + 2gq_r H + V(H)^2} \quad (2)$$

where  $\Delta T_s$  is the surface temperature deficit,  $T$  is the average temperature between the surface and height  $H$ , and  $q_r$  can be expressed as  $q_r = \frac{R}{3600\rho v_f}$  where  $\rho$  is the density of air ( $1 \text{ kg m}^{-3}$ ), and  $v_f$  is the fall velocity of precipitation ( $5 \text{ m s}^{-1}$  for rain). Based on a downdraft starting pressure of 600 hPa equal to the level of minimum equivalent potential temperature (Figure 7, see Atkins and Wakimoto), we set  $H=4218 \text{ m}$ ,  $T=3.4 \text{ K}$  and  $V(H)=31.5 \text{ kts}$ , based on the sounding in Figure 7 with a  $\Delta T_s$  equal to 4 K based on the sudden temperature drop in Figure 5, and rainfall rate of 0.17 mm/hr. Combining these into Equation 2, a gust of 57 kts is estimated, compared with an observed peak gust of 63 kts. Given that the initial momentum of the downdraft is estimated as 31.5 kts, this gives an approximately equal contribution from negative buoyancy and downwards momentum transport processes.